ASME Journal of Solar Energy Engineering
Online journal at:
https://asmedigitalcollection.asme.org/solarenergyengineering

Gustavo P. C. da Cruz
Program in Systems Engineering,
Polytechnic School of Pernambuco,
University of Pernambuco,
Recife, 50720-001 PE, Brazil
e-mail: gpcc@poli.br

Gabriel L. Barreto
Program in Systems Engineering,
Polytechnic School of Pernambuco,
University of Pernambuco,
Recife, 50720-001 PE, Brazil
e-mail: glb2@poli.br

Luis A. Gómez-Malagón
Program in Systems Engineering,
Polytechnic School of Pernambuco,
University of Pernambuco,
Recife, 50720-001 PE, Brazil
e-mail: lagomezma@poli.br

Ricardo A. de Lima[1]
Program in Systems Engineering,
Polytechnic School of Pernambuco,
University of Pernambuco,
Recife, 50720-001 PE, Brazil
e-mail: ricardo.lima@poli.br

Caio V. P. Vital
Polytechnic School of Pernambuco,
University of Pernambuco,
Recife, 50720-001 PE, Brazil
e-mail: caio.vital@poli.br

Solar Simulator Prototype With Halogen and Light-Emitting Diode Sources

Hybrid solar simulators (SS) using halogen lamps and light-emitting diodes (LEDs), classified as A for spectral match (SM) and temporal instability (TI), are primarily reported for characterizing small solar cells (160 cm^2). However, spatial nonuniformity (SNU) reports are rare. This article presents the characterization of a large-area hybrid SS capable of simulating sunlight intensity and spectrum using a combination of ten white LEDs, six halogen lamps, and 12 power LEDs being three blue (450 nm), three magenta (750 nm), and three infrared (850 nm). This setup ensures homogeneous light distribution over a 600 cm^2 surface. The proposed SS was characterized according to the International Electrotechnical Commission (IEC 60904-9) standard, analyzing SM, SNU, and TI. The obtained values (SM = 1.29, SNU = 1.5%, and TI = 0.17%) classify the simulator as BAA. Electrical characterization of a 5W solar panel (300 cm^2) was performed via current–voltage (I–V) and power–voltage (P–V) curves under indoor and outdoor conditions. A relative error of less than 4% was found compared to outdoor measurements, making it suitable for photovoltaic device testing. The results demonstrate the feasibility of developing a low-cost SS using incandescent and semiconductor light sources, with the potential for characterizing commercial photovoltaic devices. [DOI: 10.1115/1.4067972]

Keywords: hybrid solar simulator, spectral matching, spatial nonuniformity, temporal instability, photovoltaic characterization

1 Introduction

A solar simulator (SS) is an equipment that emits radiation with the intensity and spectral content of sunlight, functioning as a blackbody radiator at approximately 5800 K [1]. It is used in controlled indoor tests of photovoltaic (PV) cells, plastics, polymers, and other materials sensitive to sunlight. This equipment is standardized and classified considering three parameters: spectral match (SM), spatial nonuniformity (SNU), and temporal instability (TI). Each parameter is rated from A (most efficient) to C (least efficient), with the highest performing solar simulators being designated as AAA. These characteristics were standardized by two organizations: (i) American Society of Testing Materials (ASTM E927-10) [2] and (ii) International Electrotechnical Commission (IEC 60904-9) [3]. In terms of the spectral match, all standards have the same requirements in the range of 400–1100 nm (Class A: 0.75–1.25, Class B: 0.60–1.40, Class C: 0.4–2.0). In terms of spatial nonuniformity of irradiance, the ASTM E927-10 and IEC 60904-9 have the same requirements (Class A: 2%, Class B: 5%, Class C: 10%). In terms of temporal instability, the IEC 60904-9 defined two variables: long-term instability (LTI) and short-term instability (STI). For these two standards, the requirements are the same for the LTI (Class A: 2%, Class B: 5%, Class C: 10%) and STI (Class A: 0.5%, Class B: 2%, Class C: 10%). In the case of the ASTM E927-10, only the temporal instability is defined (Class A: 2%, Class B: 5%, Class C: 10%). Recently, the IEC 60904-9 introduced a new class called A+ with a spectral match of 0.875–1.125 in the range of 300–1200 nm, spatial nonuniformity of irradiance of 1%, LTI of 1%, and STI of 0.25% [4]. This class was created to keep up with the changes in the illumination technology using light-emitting diode (LED) and in PV solar cells such as tandem and multijunction, and also compound materials such as perovskite-Si solar cells that respond to a wider wavelength range than 400–1100 nm [5].

The choice of the light source and the definition of its positioning are crucial for the design of an SS. In first-generation high-flux solar simulators (HFSS), designed in the 1970 s, metal halide arc [6,7] and carbon arc lamps were used [8,9]. Currently, the most

[1]Corresponding author.

Contributed by the Solar Energy Division of ASME for publication in the Journal of Solar Energy Engineering: Including Wind Energy and Building Energy Conservation. Manuscript received June 25, 2024; final manuscript received February 10, 2025; published online March 13, 2025. Assoc. Editor: Ali Khounsary.

common lamps are argon [10,11], metal halide [10,11], xenon [12–15], and halogen [16–19]. For this application, the light is concentrated using elliptical and conical reflectors. In the case of elliptical reflectors, the lamp is located in the focus of the ellipse and the target is in the other [18]. To improve the light collection, a two-dimensional cone concentrator is used as a secondary concentrator [19]. For nonconcentration applications, parabolic mirrors are used. In this case, the lamp is in the focus of the parabola such that the emerging light from the reflector should be uniform [20].

Despite the excellent performance in relation to the classifications determined by IEC 60904-9, the use of these lamps presents some drawbacks. For example, the Xe arc lamp has drawbacks such as the potential to be hazardous because the gas is pressurized, change of the spectral irradiance on time enhancing the IR and reducing the UV spectral components, instability on intensity according to power instabilities, permanent mismatch due to filters, short lifetime, and cost [21]. Among the sources mentioned, the energy conversion efficiency and color temperature of metal halide, xenon, tungsten halogen, and argon lamps are 24.59%, 18.77%, 10.21%, and 3.08%, and 4000–6000 K, 6000 K, 2100–3350 K, and 6500 K, respectively [22]. It means that the spectra of lamps with color temperature close to the color temperature of the sunlight (5500–6500 K) have a better matching to the sun spectra. It is also evidenced by observing the amount of energy delivered in the IR region (>1000 nm) by metal halide, tungsten, and xenon lamps which are 32.6%, 51.3%, and 29.0%, respectively [23]. These results show that the tungsten lamp has the lowest color temperature and the highest IR amount of energy delivered among the lamps presented. Despite not having the highest efficiency among the light sources used in SS, in addition to presenting strong emission in the infrared (IR) region, the halogen lamp has attracted great attention due to its low cost among the gas lamps available for SS [24].

Research to improve the design of SS using alternative technologies has given rise to the use of LEDs [25]. The use of this light source has advantages over conventional sources. Despite LEDs have a narrow spectral emission band, they are available in a wide range of wavelengths from deep ultraviolet to near infrared. Mixing the spectral components of the LEDs, a like-sun spectra can be obtained despite that the LEDs are not continuous. Additionally, controlling the LED current, the intensity of the SS is adjusted to meet the standards. This versatility allows for greater customization and adaptability of the SS to meet a variety of specific needs [26]. Another significant advantage is the lower energy consumption of LEDs, which makes them a more sustainable and economical option in the long term. The high reliability and long lifespan of LEDs, which can reach 100,000 h in some cases, reduce the need for maintenance and frequent replacement, providing continuous and efficient operation. However, despite these advantages, full LED SS are currently applied mainly in the analysis of small area prototypes of photosensitive structures [22]. This is because, for the analyses of commercial structures such as solar PV panels and solar thermal collectors, the high cost of LEDs becomes unfeasible as the illumination area increases.

The vast majority of works described in the literature on full LED SS are class AAA. These simulators use LEDs that operate in the wavelength range between 390 and 940 nm. The quantity and optical power of each type of LED vary according to the project, being intrinsically related to the effective operating area of the simulator. For example, in the study carried out by Stuckelberger et al. [27], 11 LEDs of different wavelengths, ranging from 399 to 728 nm, were used to create an SS with an effective area of 324 cm^2. Another example is the work of Linden et al. [28], who used 23 LEDs with wavelengths between 350 and 1100 nm. These LEDs were mounted in blocks, resulting in an effective operating area of 400 cm^2. Al-Ahmad et al. [29] developed a specific SS for applications in printed organic solar cells. They used six LEDs, including warm and cool white light types, as well as LEDs with wavelengths between 478 and 1008 nm. The effective area of this simulator was 20 cm^2, suitable for accurate analysis of small samples of solar cells. Finally, Watjanatepin and Sritanauthaikorn [30] used a modular array with 15 LEDs with wavelengths ranging from 450 to 940 nm (two of 450 nm, three of 525 nm, one of 625 nm, two of 730 nm, one of 850 nm, and six of 940 nm). This arrangement resulted in an effective operating area of 416 cm^2.

Several studies have described the development of SS using halogen lamps. An example is the work of Arifin et al. [17], who implemented an ASTM Class B SS using 20 reflectors equipped with 500 W halogen lamps each, covering an operating area of 1.4 m^2. Al Sultani et al. [31] used six tungsten halogen lamps of 1 kW to provide solar radiation varying from 378 to 969 W/m^2 on an experimental area of 1200–520 mm. The characterization results indicated that the proposed SS is Class C for spatial uniformity and Class A for temporal uniformity. Rosli et al. [32] built an SS based on halogen lamps in an arrangement of 12 lamps of 500 W illuminating an area of 1.3×1.7 m^2. The characterization results according to the IEC 60904-9 revealed that the spectral match value was classified in Classes C (400–500 nm) and B (500–600 nm), and Class C for spatial nonuniformity.

In addition to pure halogen configurations, hybrid designs combining LEDs and halogen lamps are also common. Namin et al. [33] exemplify this approach using a set of six halogen lamps together with an array of 1024 blue LEDs, with a central wavelength of 468 nm. This hybrid system resulted in a BAB class SS, with an operating area of 400 cm^2. Grandi et al. [34] developed a Class B spectral matching hybrid SS with a working area of 12.5 cm × 12.5 cm. In this device, 20 power LEDs (four white warm LEDs (3700 K), four white cold LEDs (8300 K), two bluish-green LEDs (500 nm), two green LEDs (530 nm), three amber LEDs (600 nm), and five blue LEDs (470 nm)) and one halogen pin-based lamp (75 W) were chosen. Baguckis et al. [35] demonstrated that a hybrid SS based on high-power LEDs and halogen lamps can achieve the Class AAA in a usable area of at least 3 cm diameter. Bodnár et al. [36] built a low-cost SS using four LED blocks of different colors and a halogen reflector illuminating an area of 150 mm × 150 mm. According to the ASTM E972 standard, the device was classified as Class C. Chatterjee and Khandekar [37] developed a hybrid SS assembled using a high-power LED module (100 W warm-white light module) and two commercial halogen lamps (50 W) and classified it as a AAA with an area of 40×40 mm^2. Du et al. [38] designed an SS able to project a sun-like irradiance on the target surface region of 100 cm × 100 cm. Although the common standards used to classify the SS were not used, the results reported that the correlation coefficient between the measured spectrum and the reference spectrum was 0.90, the temporal instability was 3.38%, and irradiance nonuniformity was in the range 15.74–16.74% depending on the zenith angle.

Given the considerations presented, it is clear that, for the design of a low-cost SS aimed at analyzing commercial photosensitive devices, the combination of halogen sources and LEDs represents an effective and economically viable solution. Halogen lamps are particularly suitable due to their spectral content, which includes the infrared range and a luminous intensity compatible with solar radiation, equivalent to 1000 W/m^2 [16–19]. In addition to halogen lamps, the use of LED is also an interesting strategy to fill the visible spectral range that is not covered by halogen lamps to match the solar spectrum. Although LEDs usually do not allow luminosity control, they are low cost and can significantly contribute to their use with halogen lamps. As presented, hybrid SS using halogen lamps and LEDs are widely studied and classified according to the standards, and SS classified as AAA are successfully reported in the literature for small areas. However, low-cost hybrid SS with large areas are not extensively studied.

Given this scenario, this article proposes a hybrid SS (halogen + LEDs), designed to operate in an area of 600 cm^2. The system consists of a combination of ten white LEDs, six halogen lamps, and 12 power LEDs being three blue (450 nm), three magenta (750 nm), and three infrared (850 nm). To evaluate the effectiveness of the SS, detailed analyses were conducted based on the criteria of the

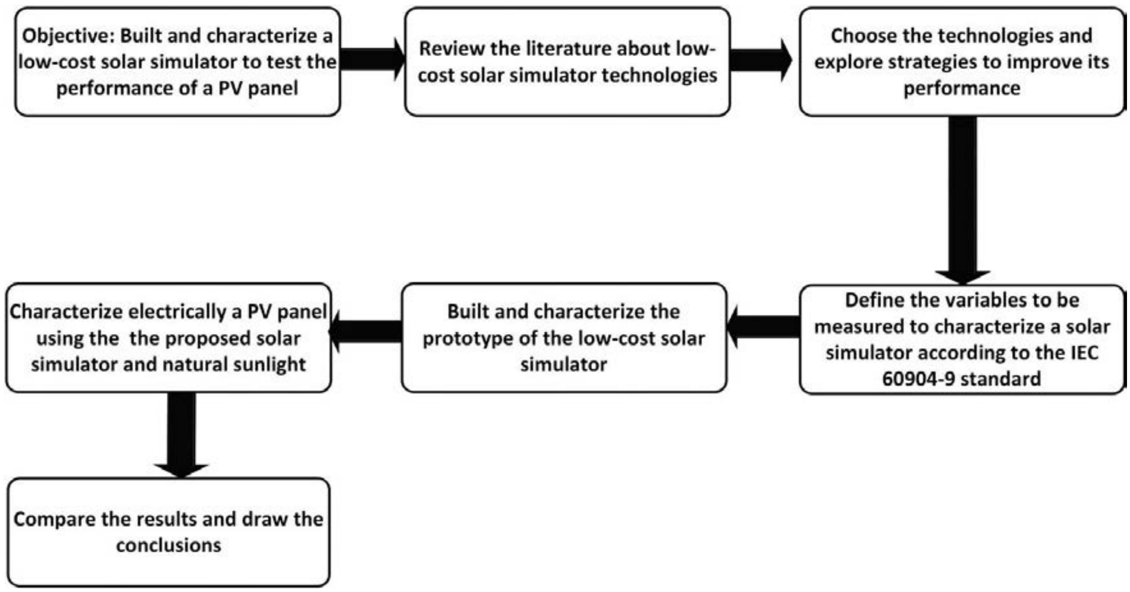

Fig. 1 Flowchart of the research carried out

IEC 60904-9 standard, which include SM, spectral nonuniformity (SNU), and TI. Based on these parameters, the proposed SS achieved the BAA rating. The results of these tests demonstrated that the proposed SS is capable of testing adequately the performance of solar panels.

2 Materials and Methods

The research presented in this article follows the flowchart shown in Fig. 1.

In our case, the hybrid technology using halogen lamps and LEDs was chosen due to the low cost of the components and the potential to be used in an SS to test PV solar panels. This session will cover the methodology for performing SS classification in accordance with the IEC 60904-9 standard and the calculation of the electrical variables for a PV solar panel using electrical parameters obtained from a curve tracer. Additionally, the construction process of the SS and the experimental setup used to achieve its classification will be detailed, along with the characterization of a 5 W solar panel.

2.1 Standard for the Analysis of Solar Simulators. SM is the ratio of the actual percentage of total irradiance to the required percentage, specified by IEC 60904-9 for each wavelength range and is calculated from the following expression:

$$SM = \frac{X_{\text{DUT},i}}{X_{\text{Ref},i}} \quad (1)$$

where the indices DUT and Ref correspond to the device under test and the air mass (AM1.5G) spectrum, respectively. The X is the percentage of the total irradiance content in the wavelength range 250–1000 nm, which is the spectral range of the simulator in the ith wavelength range, given by

$$X_{y,i} = \frac{\int_i G_y(\lambda)\,d\lambda}{\int_{300}^{1400} G_y(\lambda)\,d\lambda} \quad (2)$$

where $G_y(\lambda)$ is the spectral irradiance measured on the DUT or corresponding reference. Table 1 describes the radiation distribution for each wavelength range. As established by the standard IEC 60904-9, the classification of an SS is determined by SM as follows:

- Class A: 0.75–1.25
- Class B: 0.6–1.4
- Class C: 0.4–2.0

Table 1 Requirements for spectral matching [3]

Wavelength (nm)	Total irradiance percentage		
	AM1.5 Direct	AM1.5 Global	AM0
300–400	Not specified	Specified	8.0%
400–500	16.9%	18.4%	16.4%
500–600	19.7%	19.9%	16.3%
600–700	18.5%	18.4%	13.9%
700–800	15.2%	14.9%	11.2%
800–900	12.9%	12.5%	9.0%
900–1100	16.8%	15.9%	13.1%
1100–1400	Not specified	Not specified	12.2%

The A+ rating, as per the 2020 update of the IEC 60904-9 standard, applies to a wavelength range of 300–1200 nm. However, all tests conducted in this study were within the 400–1100 nm range, so the A+ rating criterion was not applied.

SNU is calculated as follows:

$$SNU = \left(\frac{E_{\max} - E_{\min}}{E_{\max} + E_{\min}}\right)100 \quad (3)$$

where $E_{\max}$ and $E_{\min}$ represent, respectively, the maximum and minimum intensity in the test section. SNU refers to the variation in the intensity of the light emitted by the simulator. This nonuniformity can be caused by several factors, such as irregularities in the light source, variations in the medium through which the light passes, or imperfections in the test surface. As established by the standard, the SNU classification of an SS is determined as follows:

- Class A: SNU < 2%
- Class B: SNU < 5%
- Class C: SNU < 10%

The TI refers to the fluctuation in light intensity at a particular point over a specified period. It is computed using Eq. (3) at a particular location within the area being assessed for SNU. The standard does not define a required duration for the experiment; rather, it specifies the variation in the temporal stability value calculated over the chosen time interval, which is essential

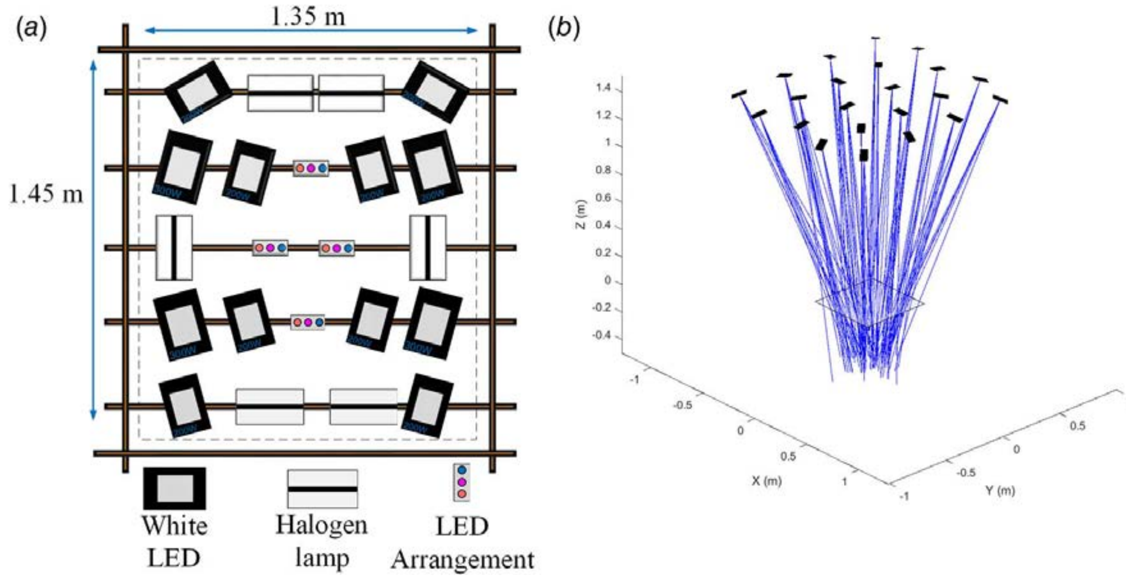

Fig. 2 (*a*) Arrangement of light sources used in the proposed SS and (*b*) ray tracing simulation for the spatial arrangement of light sources

for determining the characteristics of the photosensitive DUT. This variation in light intensity is evaluated over a short period within the total analysis time of the experiment. Class A STI SS are available on the market, with experiment durations ranging from 120 s [39] to 10 min [40].

2.2 Characterization Parameters of a Solar Panel. A method to evaluate the performance of an SS is by characterizing a solar panel, such as through obtaining the *I*–*V* and *P*–*V* curves at a specified irradiance and fixed temperature. These curves can be generated automatically using specialized equipment known as a curve tracer. Some equipment operates by varying the resistance *R* between the terminals of the solar panel to determine the operating point. From the *I*–*V* curve, the maximum power point can be obtained. This point is important for the PV system and is continuously tracked to achieve its maximum performance. Some maximum power point tracking techniques are embedded in PV inverters such as the pulse-width-modulated (PWM) DC/DC SEPIC or Cuk converter [41], the constant voltage [42,43], incremental conductance [43], fuzzy logic [44], neural networks [45], perturb and observe [46], among others. Another important parameter to be analyzed is the form factor (FF), which is given by

$$\mathrm{FF} = \frac{I_{max} V_{max}}{I_{sc} V_{oc}} \tag{4}$$

where I_{max} and V_{max}, respectively, represent the maximum current and voltage, indicating the point of maximum power, and I_{sc} and V_{oc}, respectively, represent the short circuit current and open circuit voltage.

2.3 Adopted Lighting Arrangement and Assembly of the Solar Simulator. The objective of this arrangement is to obtain a spectral filling that corresponds to the AM1.5G standard, with a luminous intensity close to that of sunlight, which is approximately 1000 W/m^2, equivalent to 124,000 lumens (lm). Figure 2(*a*) shows the spatial distribution of the light sources used in the SS design. It was made up of six 1000 W halogen lamps from the Orslam® brand, with a nominal color temperature of 2900 K [47]. These lamps were connected to a reflector with an internal aluminum coating, in order to promote more efficient targeting of the light beam. Additionally, ten 300 W white LEDs from the Foxlux® brand were incorporated into the system, with a nominal color temperature of 6500 K [48]. In addition to these main components, the arrangement includes 12 LEDs from the Epistar® brand, with an optical power of 3 W each, emitting light in the blue (450 nm), magenta (750 nm), and infrared (850 nm) bands, with four LEDs of each color [49]. These LEDs were added to fill the wavelength ranges that are not covered by LED floodlights and halogen lamps.

The alignment of the light beams was carried out using the DIALux® simulator, aiming, as can be seen in Fig. 2(*b*), to achieve a uniform distribution of the intensity and consequently, improve the classification of the SS about the SNU parameter. The final positioning for the experiments was determined by measuring the light intensity at different points on the test surface and adjustments were made to ensure a homogeneous distribution, corresponding to 1 sun, as evenly as possible.

Theoretically, activating all light sources in the array could generate around 348,000 lm, which would correspond to approximately 2.8 suns. However, measurements carried out with solar intensity instruments indicated that the array is capable of producing an intensity corresponding to 1.58 suns. This discrepancy is attributed to two main factors: the actual intensity of LED spotlights is lower than specified by manufacturers and there are thermal losses associated with halogen lamps. To adjust the intensity of the SS to a value corresponding to 1 sun, it is possible to dim the halogen lamps and adjust the polarization current of the LED arrays. It is worth noting that the LED used in this work does not have the ability to adjust intensity, as light sources with this functionality are approximately 15 times more expensive than conventional ones.

To assemble the SS, a mobile metal structure was developed to fix the light sources. This structure was manufactured by welding steel profiles, to which four casters were attached, thus allowing mobility, as illustrated in Fig. 3. The structure has a specific grid where the light sources are fixed. Strategic holes were made in the grid to allow it to be moved vertically, making it possible to adjust the light source at different heights as needed. The light sources were strategically positioned on the metallic structure in a circular configuration and capable of free horizontal rotation, with the purpose of ensuring uniform illumination across the entire test surface, allowing adjustments as necessary.

The grid was initially positioned at a height of 1.5 m from the ground, and below it, a table was placed to position the PV panel during the tests, as shown in Fig. 3. As the radiation emitted by

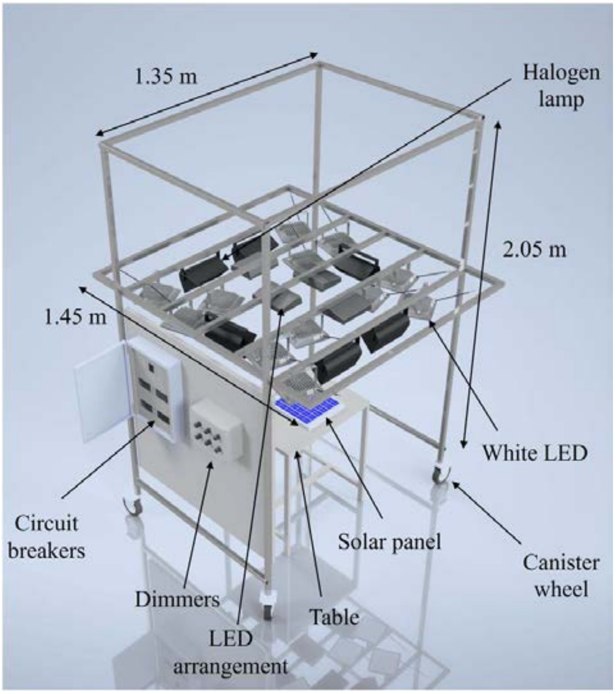

Fig. 3 Drawing of the metallic structure of the SS, with the light arrangement, protection circuits, and the dimmer for adjusting the intensity of the halogen lamps

the SS is not collimated, then the intensity varies according to the distance of the plane of test to the light source. Increasing the distance, an increase in intensity and decrease of the working area with an acceptable SNU value according to the standard are expected. The distance between the light source and the plane where the radiation was 1 sun was set to 80 cm. The entire metal structure received a special paint, with the aim of minimizing the effects of oxidation and avoiding direct contact with metal parts, prolonging the useful life of the equipment.

The sizing of the dimmer applied to halogen lamps, conductors, and circuit breakers, shown in Fig. 2, used in the SS was carried out in accordance with the standards established by NBR 5410 [50]. The section of the conductors was calculated taking into account the criteria of minimum section, current carrying capacity, and protection against overloads [50]. The main voltage is 220 V. Considering the active power supplied by the light source manufacturers and assuming that the power factor for halogen lamps and LEDs are 1 and 0.7, respectively, it can be concluded that the total active power of the system is 9714.25 W. Therefore, the total current demanded is 41.16 A. It was decided to use a three-phase power supply allowing a symmetrical distribution of active power in each phase equal to 3238.08 VA, ensuring the efficiency and safety of the simulator.

2.4 Experimental Apparatus. Figure 4 shows the schematic diagram of the experiments carried out in this article. The SM of the SS was measured using two spectrometers from StellarNet®, the BLUE-Wave VIS-50 (190–1150 nm), for the visible spectrum, and the DWARF-Star (900–1700 nm), for the infrared, as indicated in Fig. 4(*a*) The measurement is made using a fiber optic cable, which is pointed directly at the light source whose spectrum is intended to be measured. The result of the experiment can be seen graphically in real-time using the SPECTRAWIZ® program, provided by the manufacturer.

Figure 4(*b*) shows the procedure adopted to obtain experimental data to determine SNU. A calibrated reference cell model 91150 V from Newport® was used, which consists of a calibrated $2 \times 2\,cm^2$ mono-crystalline silicon solar cell. It was used to measure the irradiation intensity in an area of $2500\,cm^2$ subdivided into 25 regions of $100\,cm^2$. Due to the heat emitted by halogen lamps, measurements in demarcated areas were interrupted when the temperature in the measurement area exceeded 40 °C. This is Newport®'s recommendation to avoid loss of measurement accuracy. TI was calculated using a calibrated Kipp & Zonen® model CMP6 pyranometer, connected to a Novus® FieldLogger datalogger model (24-bit A/D converter and an acquisition speed of 1000 readings per second), as indicated in Fig. 4(*c*). The decision to use a pyranometer instead of a reference cell is due to the pyranometer's suitable encapsulation for outdoor experiments. As described in Sec. 2.1, the test duration to obtain STI classification is not clearly defined. Therefore, a duration of 5 min was established for the LTI, and about 1 min for the STI, collecting data at each 5 s, enough time to obtain the PV parameters of commercial solar panels.

For the application test on a 5 W PV panel (22 cm × 20 cm), the I_{sc}, V_{oc}, and current and voltage at the maximum power point, P_{max}, were obtained from the *I–V* and *P–V* curves using an HT Instrument Solar® I–Ve model curve tracer as shown in Fig. 4(*d*). Measurements at indoor conditions using the SS and outdoor conditions at different times (at 9.0 a.m., 10 a.m., 11 a.m., and noon) were performed. The data obtained could be examined and compared on the computer using the TOPVIEW® program, provided by the manufacturer.

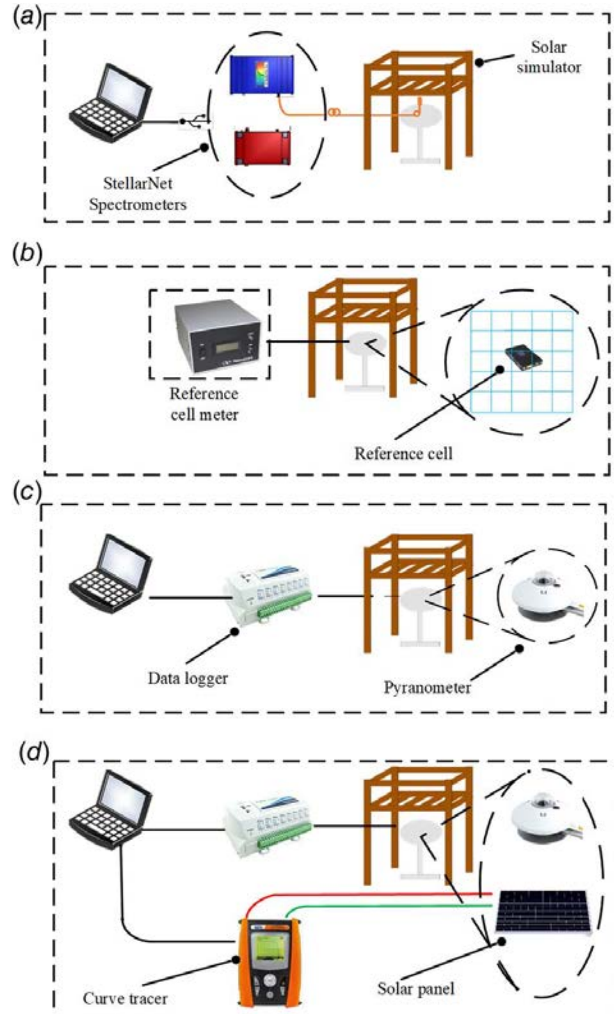

Fig. 4 Sketch of the experimental setup to obtain (*a*) spectral match, (*b*) spectral nonuniformity, (*c*) temporal instability, and (*d*) *I–V* and *P–V* curves of a solar panel

3 Results and Discussion

In this section, the results of the experiments conducted to classify the proposed SS are described. Also, the electrical response of the 5 W PV panel in indoor and outdoor conditions is analyzed. All stages were carried out at the Institute of Technological Innovation of the University of Pernambuco.

3.1 Spectral Matching. The apparatus utilized for acquiring SM data is comprehensively explained in Fig. 4(*a*). Figure 5(*a*) shows the result of the spectral analysis of the proposed SS considering the standard at AM1.5 [51]. The lighting arrangement containing only halogen lamps and LEDs resulted in a concentration of the spectrum obtained in the range of 500–700 nm. Blue (450 nm), magenta (750 nm), and infrared (850 nm) LEDs were included in the SS lighting arrangement.

Specifically, the blue LEDs were to adjust the composition of the 500–600 nm range. The magenta LED was applied for adjustments in the region between 750 and 800 nm. The spectrum above 800 nm was adjusted with LED in the infrared region. With all the necessary light sources defined and positioned, it was enough to configure the intensity of each one in order to obtain a spectral content that best complies with IEC 60904-9 in each of the desired bands.

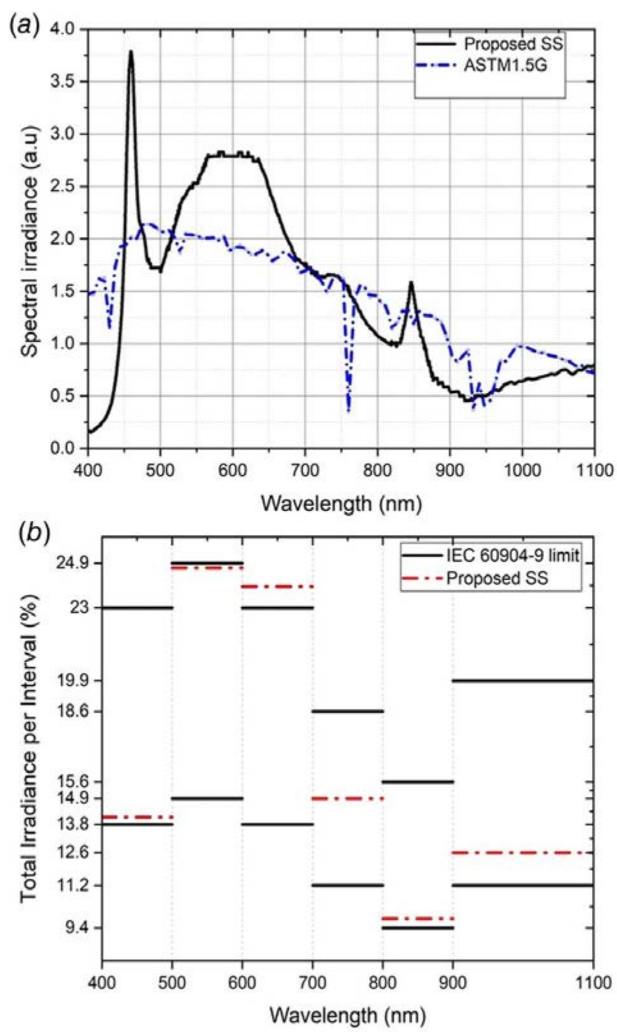

Fig. 5 (*a*) Comparison between the obtained spectra of the proposed SS at standard conditions (1 kW/m^2, 25 °C) (continuous line) and the ASTM 1.5G spectra (dashed line) and (*b*) pecentual of the irradiance at the intervals of wavelengths given by the IEC 60904-9 (continuous line) and the results obtained by the proposed SS (dashed line)

Figure 5(*b*) shows the total irradiance per wavelength range, specified by the standard and described in Table 1, and the proposed SS. In most of the wavelength ranges evaluated, the proposed SS was inside the interval given by the standard. However, in the range of 600–700 nm, the simulator presented a total irradiance range of 23.9%, resulting in an SM of 1.29. This value exceeds the maximum limit of 1.25 for Class A classification but is still within the parameters established for Class B classification. In view of the above results, the proposed SS is classified as Class B in the SM criterion.

3.2 Spatial Nonuniformity. The instrumentation adopted to obtain SNU is described in detail in Fig. 4(*b*), while the results obtained are presented in Fig. 6. The SNU analysis was performed according to the criteria established in Eq. (3) in an area of 2500 cm^2. This process resulted in an SNU value of 4.6%, which gives the classification B for the SS. When considering a smaller area, specifically 20×30 cm, where the maximum recorded intensity is 1.03 and the minimum intensity is 1 sun, an SNU value of 1.5% is obtained. This measurement falls under the classification of A. It is important to note that the 600 cm^2 area is equivalent to the surface of solar panels with a power of up to 10 W.

3.3 Temporal Instability. The equipment used to measure TI is thoroughly detailed in Fig. 4(*c*). For this study, a 5-min long-term time interval was selected, which is adequate, for instance, to obtain *I*–*V* and *P*–*V* curves of a solar panel, with the short-term interval set at 1 min, starting after the light sources have been on for 2 min. During the entire period of the experiment, the maximum and minimum intensity values recorded were, respectively, 1099 W/m^2 and 1089 W/m^2, as can be seen in Fig. 7(*a*). This intensity variation in 5 min results in a long-term TI of 0.8%, ranking SS an A in this regard. For the short-term TI analysis, according to Fig. 7(*b*), the maximum and minimum intensity values were, respectively, 1095 W/m^2 and 1093 W/m^2. This intensity variation in 1 min implies an STI of 0.17%, also classifying the SS as Class A.

3.4 Characterization of Solar Panels. The methodology employed to achieve the characterization of solar panels is outlined in Fig. 4(*d*). The I_{sc}, V_{oc}, and P_{max} were extracted from the *I*–*V* curve. The average solar irradiance during the outdoor experiments was 930 W/m^2, monitored over a 5-min time interval. The temperature set by the equipment was 25 °C. Figures 8(*a*) and 8(*b*) present,

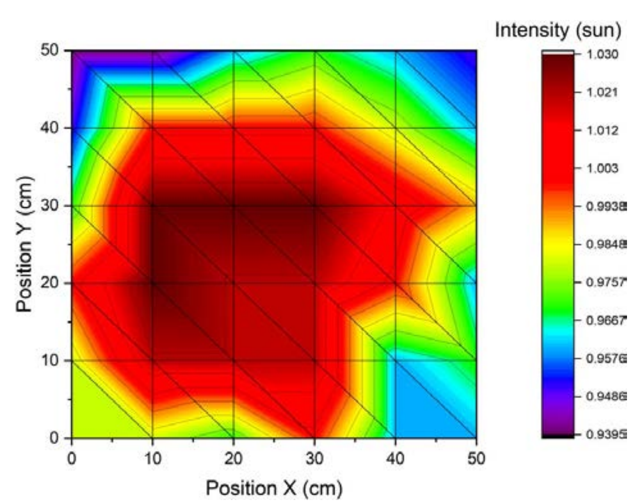

Fig. 6 Distribution of the light intensity emitted by the SS over the 2500 cm^2 test surface. Results were obtained at 1 kW/m^2 ($z = 80$ cm from the light source to the test surface).

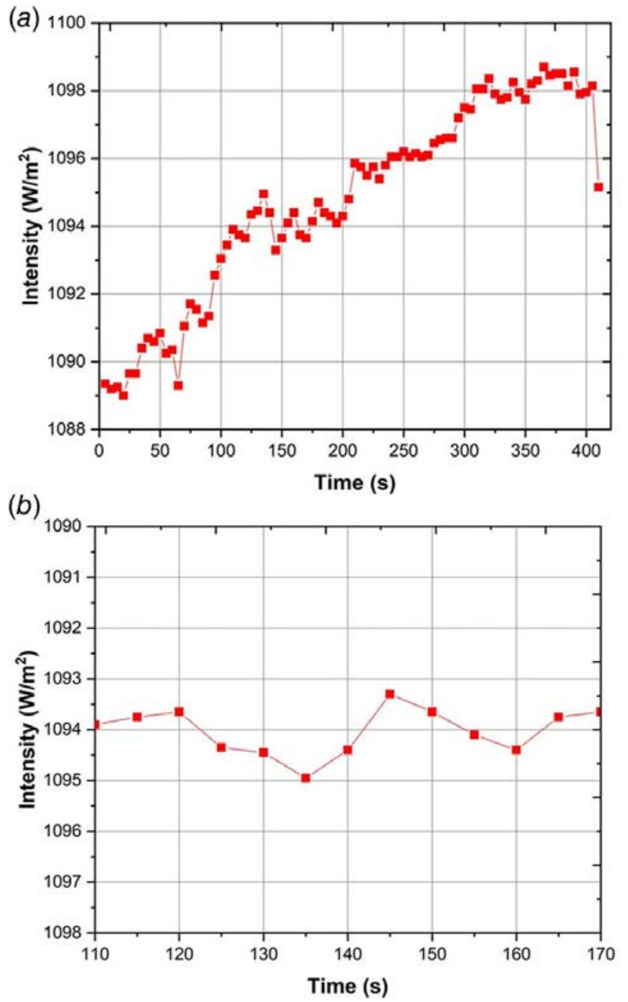

Fig. 7 Temporal instability analyzed for a period of (*a*) 5 min and (*b*) 1 min. Experiment carried out on the *XY* plane of 2500 cm^2 and 1 kW/m^2 (z = 80 cm from the light source to the test surface).

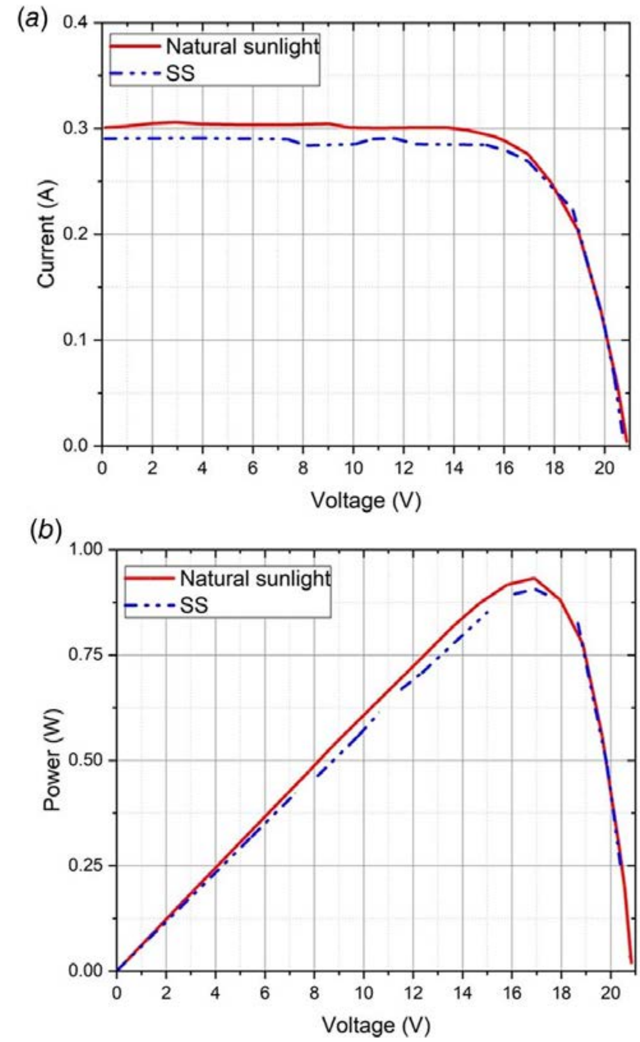

Fig. 8 Comparative analysis of the characteristic curves of the solar panel used in the experiments obtained under direct sunlight (continuous line) and SS (dashed line) at 1 kW/m^2 and 25 °C. (*a*) *I–V* curve and (*b*) *P–V* curve.

respectively, the *I–V* and *P–V* curves of the solar panel in the experiments carried out in outdoor conditions by natural sunlight and indoor conditions by the SS.

Table 2 shows the results of the parameters extracted from the curves obtained. It can be seen from Table 2 that the error was less than 4% in all parameters, indicating that the SS is suitable for carrying out the electrical characterization of PV panels. The error was calculated using the outdoor measurement as a reference.

As shown, the main findings of this work were the building and characterization of a hybrid SS, and also the indication of its use as a source light to characterize electrically a PV panel. In particular, a hybrid SS based on halogen lamps, and white and colored LEDs, illuminating an area of 600 cm^2, was built and characterized according to the IEC 60904-9 standard. The characterization results indicated that the SS is classified as Class BAA or Class B. An application example of the hybrid SS was its use in the electrical characterization of a 5 W PV panel, and the obtained results were compared to the electrical response of the PV panel under natural sunlight. A maximum error of 3.7% was observed for the short circuit current. In comparison with other Class B hybrid SS reported in the literature, the illuminating area of the proposed SS (600 cm^2) is larger than 400 cm^2 [33] and 12.5–12.5 cm^2 [34]. However, due to the limited illuminating area of the proposed prototype, its application is indicated for the characterization of solar devices with an area less than 660 cm^2 as in the case of a 5 W PV solar panel. Despite the restricted area of the proposed prototype, the finding results indicate that the hybrid technology (halogen lamp + LEDs) is suitable for the characterization of solar devices with large areas. Another important aspect is the cost of the prototype. The material cost was about US$ 920. For comparison, an SS Class AAA with a maximum beam diameter of 50 mm costs approximately 10 times more [52]. This cost difference indicates that the proposed device is a low-cost hybrid SS.

Table 2 Parameters of the *I–V* and *P–V* curves obtained in the experiments

	P_{max} (W)	V_{oc} (V)	V_{max} (V)	I_{max} (A)	I_{sc} (A)	FF
Simulator	4.47	20.75	16.93	0.26	0.29	0.74
Outdoor	4.60	20.91	16.93	0.27	0.30	0.73
Error (%)	2.83	0.77	0.0	3.7	3.33	1.4

4 Conclusion

In this work, the feasibility of building an SS with a lighting area of 600 cm^2 with BAA classification was verified, using halogen lamps, white LED, and a set of power colored LEDs. In comparison with other reports in the literature, the present work showed a hybrid

SS with a large illuminating area suitable for the characterization of commercial PV panels. Also, the approach of applying filament light sources in sets with semiconductor light sources enabled a low-cost project. Despite the area limitations and the spectral performance, the proposed device proved to be useful in the electrical characterization of a 5 W PV solar panel.

In order to improve the performance of the hybrid SS, some technical issues must be addressed. One of the limitations of the proposed simulator is the limited adjustment of light intensity. This is because the white LED spotlights used in this project are not dimmable. Therefore, the proposal for future work is to replace these to create an automatable lighting system. Halogen lamps will have their intensities adjusted by digital potentiometers, and the LED arrays can be controlled via PWM. To automate this lighting arrangement, a microprocessor platform with a resident program will be used, equipped with a user-friendly dashboard for interactive control of intensities for each wavelength range required by the standard. Including these adjustments, the SS will be able to adapt it to the new additional parameters proposed by the IEC in 2020, which are spectral coverage and spectral deviation [4]. These parameters were created to guarantee an even greater similarity of the simulated spectrum with that defined by AM1.5. The findings of this work will lead to the development of hybrid SS to be used in the characterization of common industrial solar devices such as PV panels or solar collectors with large areas.

Acknowledgment

The authors gratefully acknowledge the financial support given by the Higher Education Personnel (10.13039/501100002322 CAPES), financial code 001, Brazil.

Conflict of Interest

There are no conflicts of interest.

Data Availability Statement

The datasets generated and supporting the findings of this article are obtainable from the corresponding author upon reasonable request.

Nomenclature

E = radiation intensity (W)
I = electric current (A)
P = power (W)
V = voltage (V)
G_y = spectral irradiance ($\mathrm{W\,m^{-2}}$)

Superscripts and Subscripts

DUT = device under test
i = wavelength range
max = maximum
max = minimum
oc = open circuit
Ref = reference
sc = short circuit

Abbreviations

AM = air mass
ASTM = American Society of Testing Materials
CV = constant voltage
HFSS = high-flux solar simulators
LTI = long-term instability
MPPT = maximum power point tracking
PV = photovoltaic
SS = solar simulator
STI = short-term instability

Dimensionless Groups

FF = form factor (VA/VA)
SNU = spatial nonuniformity ($\mathrm{W\,m^{-2}/W\,m^{-2}}$)
SM = spectral match ($\mathrm{W\,m^{-2}/W\,m^{-2}}$)
TI = temporal instability ($\mathrm{W\,m^{-2}/W\,m^{-2}}$)
X = percentage of the total irradiance ($\mathrm{W\,m^{-2}/W\,m^{-2}}$)

References

[1] Emery, K., 1986, "Solar Simulators and *I–V* Measurement Methods," Solar Cells, **18**(3–4), pp. 251–260.
[2] ASTM, 2019, "Standard Classification for Solar Simulators for Electrical Performance Testing of Photovoltaic Devices," Technical Report No. E927-19, ASTM International.
[3] IEC, 2007, "Photovoltaic Devices—Part 9: Solar Simulator Performance Requirements," Technical Report No. 60904-9, International Electrotechnical Commission.
[4] International Electrotechnical Commission, 2020, "Photovoltaic Devices—Part 9: Solar Simulator Performance Requirements," Technical Report IEC 60904-9, International Electrotechnical Commission.
[5] Watjanatepin, N., Boonmee, C., Kaisookkanatorn, P., Sritanauthaikorn, P., Wannakam, K., and Thongkullaphat, S., 2023, "Light Sources and Irradiance Spectrum of Led Solar Simulator for Photovoltaic Devices: A Review," Int. J. Renew. Energy Res., **13**(1), pp. 192–207.
[6] Dong, X., Sun, Z., Nathan, G. J., Ashman, P. J., and Gu, D., 2015, "Time-Resolved Spectra of Solar Simulators Employing Metal Halide and Xenon Arc Lamps," Sol. Energy, **115**, pp. 613–620.
[7] Zhang, Y., Shaw, M., Ekman, B., Brooks, G., Rhamdhani, M. A., and Guo, C., 2024, "Characterization and Deviation Analysis of a High-Flux Solar Simulator With Metal-Halide Lamps," ASME J. Sol. Energy Eng., **146**(2), p. 021002.
[8] Esen, V., Sağlam, Ş., and Oral, B., 2017, "Light Sources of Solar Simulators for Photovoltaic Devices: A Review," Renew. Sustain. Energy Rev., **77**, pp. 1240–1250.
[9] Wang, W., and Laumert, B., 2014, "Simulate a 'Sun' for Solar Research: A Literature Review of Solar Simulator Technology," KTH Royal Institute of Technology.
[10] Gallo, A., Marzo, A., Fuentealba, E., and Alonso, E., 2017, "High Flux Solar Simulators for Concentrated Solar Thermal Research: A Review," Renew. Sustain. Energy Rev., **77**, pp. 1385–1402.
[11] Bader, R., Levêque, G., Haussener, S., and Lipiński, W., 2016, "High-Flux Solar Simulator Technology," *Optics for Solar Energy*, Optica Publishing Group, Leipzig, Germany, pp. 1–3.
[12] Li, X., Chen, J., Lipiński, W., Dai, Y., and Wang, C.-H., 2020, "A 28 Kwe Multi-source High-Flux Solar Simulator: Design, Characterization, and Modeling," Sol. Energy, **211**, pp. 569–583.
[13] Krueger, K. R., Lipiński, W., and Davidson, J. H., 2013, "Operational Performance of the University of Minnesota 45 Kwe High-Flux Solar Simulator," Proceedings of the ASME 2012 International Conference on Energy Sustainability, ASME, pp. 1093–1099.
[14] Wang, W., Aichmayer, L., Garrido, J., and Laumert, B., 2017, "Development of a Fresnel Lens Based High-Flux Solar Simulator," Sol. Energy, **144**, pp. 436–444.
[15] Zhu, Q., Xuan, Y., Liu, X., Yang, L., Lian, W., and Zhang, J., 2020, "A 130 kwe Solar Simulator With Tunable Ultra-high Flux and Characterization Using Direct Multiple Lamps Mapping," Appl. Energy, **270**, pp. 115–165.
[16] Enaganti, P. K., Dwivedi, P. K., Srivastava, A. K., and Goel, S., 2020, "Analysis of Submerged Amorphous, Mono- and Poly-crystalline Silicon Solar Cells Using Halogen Lamp and Comparison With Xenon Solar Simulator," Sol. Energy, **211**, pp. 744–752.
[17] Arifin, Z., Kuncoro, I. W., and Hijriawan, M., 2021, "Solar Simulator Development for 50 wp Solar Photovoltaic Experimental Design Using Halogen Lamp," Int. J. Heat Technol., **39**(6), pp. 1741–1747.
[18] Soetedjo, A., Nakhoda, Y. I., Lomi, A., and Suryanto, T. A., 2016, "Solar Simulator Using Halogen Lamp for PV Research," Proceedings of Second International Conference on Electrical Systems, Technology and Information 2015 (ICESTI 2015), Springer, pp. 239–245.
[19] Aksoy, F., Karabulut, H., Çınar, C., Solmaz, H., Özgören, Y. Ö., and Uyumaz, A., 2015, "Thermal Performance of a Stirling Engine Powered by a Solar Simulator," Appl. Therm. Eng., **86**, pp. 161–167.
[20] Petrasch, J., Coray, P., Meier, A., Brack, M., Haeberling, P., Wuillemin, D., and Steinfeld, A., 2007, "A Novel 50 kw 11,000 Suns High-Flux Solar Simulator Based on an Array of Xenon Arc Lamps," ASME J. Sol. Energy Eng., **129**(4), pp. 405–411.
[21] Leary, G., Switzer, G., Kuntz, G., and Kaiser, T., 2016, "Comparison of Xenon Lamp-Based and LED-Based Solar Simulators," 2016 IEEE 43rd Photovoltaic Specialists Conference (PVSC), IEEE, pp. 3062–3067.
[22] Kim, K. A., Dostart, N., Huynh, J., and Krein, P. T., 2014, "Low-Cost Solar Simulator Design for Multi-junction Solar Cells in Space Applications," Power and Energy Conference at Illinois (PECI), IEEE, pp. 1–6.
[23] Krusi, P., and Schmid, R., 1983, "The CSI 1000 W Lamp as a Source for Solar Radiation Simulation," Sol. Energy, **30**(5), pp. 455–462.

[24] Tawfik, M., Tonnellier, X., and Sansom, C., 2018, “Light Source Selection for a Solar Simulator for Thermal Applications: A Review,” Renew. Sustain. Energy Rev., **90**, pp. 802–813.
[25] Lopez-Fraguas, E., Sánchez-Pena, J. M., and Vergaz, R., 2019, “A Low-Cost LED-Based Solar Simulator,” IEEE Trans. Instrum. Meas., **68**(12), pp. 4913–4923.
[26] Chojniak, D., Bett, A. J., Hohl-Ebinger, J., Reichmuth, S. K., Schachtner, M., and Siefer, G., 2023, “LED Solar Simulators—A Spectral Adjustment Procedure for Tandem Solar Cells,” AIP Conf. Proc., **2826**(1), pp. 1–8.
[27] Stuckelberger, M., Perruche, B., Bonnet-Eymard, M., Riesen, Y., Despeisse, M., Haug, F.-J., and Ballif, C., 2014, “Class AAA LED-Based Solar Simulator for Steady-State Measurements and Light Soaking,” IEEE J. Photovoltaics, **4**(5), pp. 1282–1287.
[28] Linden, K. J., Neal, W. R., and Serreze, H. B., 2014, “Adjustable Spectrum LED Solar Simulator,” *Light-Emitting Diodes: Materials, Devices, and Applications for Solid State Lighting XVIII*, Vol. 9003, SPIE, pp. 109–117.
[29] Al-Ahmad, A. Y., Holdsworth, J., Vaughan, B., Sharafutdinova, G., Zhou, X., Belcher, W. J., and Dastoor, P. C., 2019, “Modular LED Arrays for Large Area Solar Simulation,” Prog. Photovoltaics: Res. Appl., **27**(2), pp. 179–189.
[30] Watjanatepin, N., and Sritanauthaikorn, P., 2022, “Rectangular Module for Large Scale Solar Simulator Based on High-Powered LEDs Array,” TELKOMNIKA (Telecommun. Comput. Electron. Control), **20**(2), pp. 462–474.
[31] Al Sultani, K., Al Shuaili, A., Al Adawi, A., Husain, A., Ansari, M. Z., and Zunaid, M., 2024, “Optimization of Lamps Configuration for a Large-Scale Indoor Solar Simulator for PV Panels and Solar Collectors,” J. Adv. Res. Appl. Mech., **123**(1), pp. 195–205.
[32] Rosli, M. A. M., Hamizan, M. A. D., Nawam, M. Z., Hussain, F., and Herawan, S. G., 2022, “Measurement of Spectral Match and Spatial Non-uniformity for Indoor Solar Simulator,” J. Adv. Res. Fluid Mech. Therm. Sci., **100**(1), pp. 98–115.
[33] Namin, A., Jivacate, C., Chenvidhya, D., Kirtikara, K., and Thongpron, J., 2012, “Construction of Tungsten Halogen, Pulsed LED, and Combined Tungsten Halogen-LED Solar Simulators for Solar Cell-Characterization and Electrical Parameters Determination,” Int. J. Photoenergy, **2012**(1), p. 527820.
[34] Grandi, G., Ienina, A., and Bardhi, M., 2014, “Effective Low-Cost Hybrid LED-Halogen Solar Simulator,” IEEE Trans. Ind. Appl., **50**(5), pp. 3055–3064.
[35] Baguckis, A., Novičkovas, A., Mekys, A., and Tamošiūnas, V., 2016, “Compact Hybrid Solar Simulator With the Spectral Match Beyond Class A,” J. Photonics Energy Soc. Photo-Opt. Instrum. Eng., **6**(3), p. 035501.
[36] Bodnár, I., Koós, D., Iski, P., and Skribanek, Á., 2020, “Design and Construction of a Sun Simulator for Laboratory Testing of Solar Cells,” Acta Polytech. Hungarica, **17**(3), pp. 165–184.
[37] Chatterjee, D., and Khandekar, S., 2023, “Hybrid Solar Simulator for Long-Term Testing of Photothermal Materials,” IEEE Trans. Instrum. Meas., **72**, pp. 1–8.
[38] Du, Z., Zhao, H., Jia, G., and Li, X., 2023, “Design, Fabrication, and Evaluation of a Large-Area Hybrid Solar Simulator for Remote Sensing Applications,” Opt. Express, **31**(4), pp. 6184–6202.
[39] Newport, 2024, “Sol3A Class AAA Solar Simulators,” https://www.newport.com/f/class-aaa-solar-simulators, Accessed May 30, 2024.
[40] Eternal, 2024, “Manufacturing Solar Simulators,” https://www.eternalsun.com/product/manufacturing-solar-simulators, Accessed May 30, 2024.
[41] Chung, H.-H., Tse, K., Hui, S. R., Mok, C., and Ho, M., 2003, “A Novel Maximum Power Point Tracking Technique for Solar Panels Using a Sepic or Cuk Converter,” IEEE Trans. Power Electron., **18**(3), pp. 717–724.
[42] Tozlu, Ö. F., and Çalık, H., 2021, “A Review and Classification of Most Used MPPT Algorithms for Photovoltaic Systems,” Hittite J. Sci. Eng., **8**(3), pp. 207–220.
[43] Sarvi, M., and Azadian, A., 2022, “A Comprehensive Review and Classified Comparison of MPPT Algorithms in PV Systems,” Energy Syst., **13**, pp. 281–320.
[44] Sarikh, S., Raoufi, M., Bennouna, A., and Ikken, B., 2021, “Characteristic Curve Diagnosis Based on Fuzzy Classification for a Reliable Photovoltaic Fault Monitoring,” Sustain. Energy Technol. Assess., **43**, p. 100958.
[45] Sayyad, J., and Nasikkar, P., 2021, “Design and Development of Low Cost, Portable, On-Field IV Curve Tracer Based on Capacitor Loading for High Power Rated Solar Photovoltaic Modules,” IEEE Access, **9**, pp. 70715–70731.
[46] Zhu, Y., and Xiao, W., 2020, “A Comprehensive Review of Topologies for Photovoltaic *I–V* Curve Tracer,” Sol. Energy, **196**, pp. 346–357.
[47] Osram, 2024, “Halogen Lamp,” https://www.osram.com/cb/, Accessed May 30, 2024.
[48] Foxlux, 2024, “LED Reflector,” https://www.foxlux.com.br/produto/refletor-led/, Accessed May 30, 2024.
[49] Epistar, 2024, “LED,” https://www.ledestar.com/product-daohanglan/, Accessed May 30, 2024.
[50] Associação Brasileira de Normas Técnicas, 2004, “Norma Brasileira de Instalações Elétricas de Baixa Tensão—NBR 5410,” Norma Brasileira NBR 5410, Norma Técnica, ABNT, Rio de Janeiro.
[51] National Renewable Energy Laboratory, 2024, “Reference Air Mass 1.5 Spectra,” https://www.nrel.gov/grid/solar-resource/spectra-am1.5.html
[52] Holmarc, 2024, “Solar Simulator,” https://www.holmarc.com/solar_simulator1.php, Accessed September 19, 2024.